Closed-Loop Neuromuscular Electrical Stimulation Method Provides Robustness to Unknown Time-Varying Input Delay in Muscle Dynamics

Serhat Obuz, Victor H. Duenas, Ryan J. Downey, Justin R. Klotz, and Warren E. Dixon

***Abstract*— Neuromuscular electrical stimulation (NMES) is commonly used to rehabilitate people with motor impairment (e.g., following stroke or spinal cord injury). Closed-loop NMES holds the promise to facilitate coordinated limb motion, but technical challenges remain. In particular, there is a potentially destabilizing delay between the application of the electrical stimulation and the ensuing muscle contraction, which changes as muscle fatigues. In this brief, a closed-loop NMES method is developed to yield lower limb tracking, despite an unknown time-varying input delay, uncertain nonlinear limb dynamics, and additive bounded disturbances. A novel filtered error signal is designed using the past states in a finite integral over a constant estimated delay interval. The control development is based on an approach that uses Lyapunov–Krasovskii functionals in a Lyapunov-based stability analysis to prove ultimately bounded tracking. Experimental results in healthy individuals and participants with neurological conditions are provided to demonstrate the performance of the developed controller.**

***Index Terms*— Delay systems, Lyapunov methods, neuromuscular electrical stimulation (NMES), nonlinear control systems, robust control, uncertain systems, unknown time-varying input delay.**

I. Introduction

NEUROMUSCULAR electrical stimulation (NMES) evokes muscle contractions by applying an external electrical stimulus. Challenges of closed-loop NMES control are related to the unknown and nonlinear mapping from electrical input to generated muscle force [1], muscle force decay under a constant stimulation intensity because of fatigue [2], uncertain parameters and unmodeled disturbances in the dynamic model [3], and the delayed muscle response to electrical stimulation [4]. Another challenge related to the delayed muscle response, which is modeled as an input delay, is that this delay is time-varying due to muscle fatigue [5], [6].

Closed-loop NMES [or functional electrical stimulation (FES)] control has been applied in several applications [7]. In [8], iterative learning control (ILC) with a model identification procedure was implemented with passive robotic assistance for upper-limb tracking tasks with people with multiple sclerosis. In [9] and [10], ILC was implemented for foot trajectory tracking during the swing phase in the gait using a drop foot neuroprosthesis. The delay in the system dynamics is addressed by adding a time shift in the controller developed in [9] and [10]. In [11], the quadriceps and hamstrings were stimulated to reduce the torque contribution of a powered exoskeleton during locomotion of three paraplegics. The result in [11] concluded that the muscles exhibited delays ranging from 75 to 200 ms; however, no delay compensation was provided. In [12], a review examined recent advances in closed-loop control and sensing techniques for FES standing following spinal cord injury (SCI). However, a prevalent challenge in muscle motion control is the time-delayed muscle activation [13] that affects torque generation potentially leading to a destabilizing effect in human motor control tasks [6], [14]. Hence, there is a need for a closed-loop NMES controller to track the desired limb motion that is robust to the unknown time-varying input delay effects and uncertain nonlinear muscle dynamics.

Input time-delayed systems and the associated stability analysis have been extensively studied in recent years [15]. In particular, various results (see [16]–[33]) have developed controllers for nonlinear systems with an input time delay. In results such as those in [16]–[19], it is assumed that the input time-delay is known with exact model knowledge of the nonlinear dynamics. Results such as those in [20]–[25] focus on the development of non-model-based controllers for an uncertain nonlinear system with a known input delay. Since measurement of the input delay can be problematic in many practical engineering applications, results such as those in [26]–[33] are available for nonlinear systems with an unknown input delay. However, results such as those in [26]–[30] explicitly rely on the exact model knowledge of the nonlinear systems. As an alternative, robust control methods are developed in [31]–[33] for general uncertain nonlinear systems (not specific to NMES/FES). In [31], the control development assumes that the input delay is constant and uncertain. The controller in [32] is designed for uncertain nonlinear systems based on the assumption that the input delay is unknown and slowly varying.

Recently, NMES controllers have considered the delayed response of muscle [34]–[42]. The results in [34] and [35] ensure uniformly ultimately bounded tracking despite uncertain dynamics with additive disturbances, but the input delay is assumed to be known and constant. Although the stability analysis of the controller designed in [35] requires

Manuscript received April 26, 2018; revised November 14, 2018; accepted June 4, 2019. Date of publication July 30, 2019; date of current version October 9, 2020. Manuscript received in final form June 28, 2019. This work was supported in part by NSF under Award 1762829. Recommended by Associate Editor B. Jayawardhana. *(Corresponding author: Serhat Obuz.)*

S. Obuz is with the Department of Electrical and Electronics Engineering, Eskişehir Osmangazi University, Eskişehir 26040, Turkey (e-mail: sobuz@ogu.edu.tr).

V. H. Duenas and W. E. Dixon are with the Department of Mechanical and Aerospace Engineering, University of Florida, Gainesville, FL 32611 USA (e-mail: vhduenas@ufl.edu; wdixon@ufl.edu).

R. J. Downey is with the College of Health Professions, Medical University of South Carolina, Charleston, SC 29425 USA (e-mail: downeyr@musc.edu).

J. R. Klotz is with the Department of Defense, Huntsville, AL 35898 USA (e-mail: jklotz.controls@gmail.com).

Color versions of one or more of the figures in this article are available online at http://ieeexplore.ieee.org.

Digital Object Identifier 10.1109/TCST.2019.2926945

exact knowledge of the input delay, the experimental studies demonstrate that the controller is robust to some uncertainty in the delay. In [36], a controller is designed to switch between the stimulations of the agonist and antagonist muscles instead of stimulating only agonist muscles to reduce tracking error. The proposed controller in [37] considers the activation dynamics as a means to improve position tracking. However, the control development proposed in [36] and [37] assumes exact knowledge of a constant input delay. Motivated by the desire to provide robustness to uncertainty in the delayed force production of electrically stimulated muscle, a global asymptotic tracking controller was developed in [38] under the assumptions of the exact model knowledge of the lower limb dynamics and an unknown constant delay. The controller in [39] compensates for known time-varying input delay disturbances while tracking a reference force during isometric NMES. The controller in [40] assumes a known time-varying input delay in the control structure to compensate for the input delay effects in the closed-loop dynamics to track a reference position in NMES. The model-free controllers in [39] and [40] assume the exact knowledge of the input delay is available. The controller in [41] is designed to compensate for an unknown time-varying input delay and disturbances for force tracking in isometric NMES. The result in [42] ensures uniformly ultimately bounded position tracking for NMES for an unknown time-varying input delay; however, it assumes that the time-varying delay rate is less than 1. As an alternative, a controller is developed in [33] for uncertain Euler–Lagrange dynamics to compensate for an unknown time-varying input delay; in addition, the controller does not require the knowledge of the delay rate and relaxes the assumption on the delay rate in [42].

This brief builds on our precursory results in [33] and [42] by adding an integral feedback of the error signal to increase the tracking performance and robustness of the controller with respect to parametric uncertainty, unmodeled disturbances, and effects of the unknown time-varying input delay. The newly designed delay-compensating controller provides an exponential decay rate of the tracking error to an ultimate bound. Experimental results obtained from ten able-bodied individuals and three participants with neurological conditions (NCs) illustrate the performance of the controller, beyond the modified stability analysis. The key contributions of the controller include compensating for an unknown time-varying input delay, rather than assuming that the delay is constant and known [34], [35] and compensating for the uncertain nonlinear limb dynamics by using the past states of the controller in a finite integral over an estimated delay interval in the control structure. Another contribution is that the maximum allowable mismatch between the actual input delay and the estimated input delay is obtained to guarantee tracking. Since the approximate interval of the time-varying input delay can be experimentally obtained for NMES [39], the estimated delay can be selected to minimize the mismatch between the actual input delay and the estimated input delay. A Lyapunov-based stability analysis is used to prove uniformly ultimately bounded tracking.

II. Knee Joint Dynamics

The single degree-of-freedom musculoskeletal knee-joint dynamics are modeled as [43]

$$M(q,\dot{q})\ddot{q} + f(q,\dot{q}) + d(t) = u(t-\tau(t)) \tag{1}$$

where $q, \dot{q}, \ddot{q} \in \mathbb{R}$ symbolize the angular position, velocity, and acceleration of the shank about the knee-joint, respectively. In (1), $M : \mathbb{R}\times\mathbb{R} \to \mathbb{R}$ and is defined as $M \triangleq (J/\Omega\xi\zeta)$, where $J \in \mathbb{R}$ is an uncertain positive constant denoting the inertia of the shank and the foot, $\Omega : [t_0,\infty) \to \mathbb{R}$ denotes an unknown positive time-varying function exhibiting skeletal muscle fatigue and potentiation, $\xi : \mathbb{R}\times\mathbb{R} \to \mathbb{R}$ is a sufficiently smooth, unknown nonlinear function that depends on the knee-joint angle and angular velocity [43], which is bounded and positive, provided the muscle is not fully stretched or contracting concentrically at its maximum shortening velocity [44], $\zeta : \mathbb{R} \to \mathbb{R}$ is a positive moment arm that changes with the extension and flexion of the leg [45], [46]. Also in (1), the nonlinear function $f : \mathbb{R}\times\mathbb{R} \to \mathbb{R}$ and is defined as $f \triangleq (1/\Omega\xi\zeta)(k_1\exp(-k_2 q)(q-k_3) + mgl\sin(q) - B_1\tanh(-B_2\dot{q}) + B_3\dot{q})$, where $k_1, k_2, k_3, m, g, l, B_1, B_2, B_3 \in \mathbb{R}$ are uncertain positive constants, where m is the combined mass of the shank and the foot, g is the gravitational acceleration, and l is the distance between the knee-joint and the lumped center of the mass of the shank and the foot, $k_1\exp(-k_2 q)(q-k_3)$ denotes the elastic effects, $mgl\sin(q)$ denotes the effects due to gravity, and $B_1\tanh(-B_2\dot{q})$ symbolizes the viscous and $B_3\dot{q}$ denotes the damping effects [43], [47]. The dynamics in (1) also include a sufficiently smooth unknown time-varying exogenous disturbance (e.g., unmodeled dynamics) defined as $d : [t_0,\infty) \to \mathbb{R}$, where $t_0 \in \mathbb{R}$ is the initial time. The delayed voltage potential across the quadriceps muscle in (1) is denoted by $u(t-\tau) \in \mathbb{R}$, where $\tau : [t_0,\infty) \to \mathbb{R}$ denotes the electromechanical delay, which is the delay between the application of voltage and the onset of muscle force production, which results in torque produced about the knee-joint [47], [48]. Throughout this brief, delayed functions are symbolized as

$$h_\tau \triangleq \begin{cases} h(t-\tau) & t-\tau \geq t_0 \\ 0 & t-\tau < t_0 \end{cases}$$

where $t \in \mathbb{R}$ is the time. The subsequent control development and stability analysis exploits the following assumptions.

Assumption 1: The moment arm ζ and the functions ξ, Ω are assumed to be positive and bounded along their first and second time derivatives [45], [46], [49], [50]. Therefore, the function M in (1) can be bounded as $\underline{m} \leq |M(q,\dot{q})| \leq \overline{m}$ for all $q, \dot{q} \in \mathbb{R}$, where $\underline{m}, \overline{m} \in \mathbb{R}$ are known positive constants. Furthermore, the function f and its first partial derivative are bounded, since $\zeta, \xi, \Omega \in \mathcal{C}^2$ (i.e., twice continuously differentiable).

Assumption 2: The nonlinear additive disturbance and its first and second time derivatives exist and are bounded by known positive constants [51].

Assumption 3: The reference trajectory $q_r \in \mathbb{R}$ is designed such that q_r, $\dot{q}_r$, $\ddot{q}_r$ exist and are bounded by known positive constants.

Assumption 4: The mismatch between the actual input delay $\tau(t)$ and the constant estimated input delay $\hat{\tau} \in \mathbb{R}$ is bounded by a known constant $\bar{\bar{\tau}} \in \mathbb{R}$ such that $\sup_{t\in\mathbb{R}}|\tau - \hat{\tau}| \leq \bar{\bar{\tau}}$. Furthermore, it is assumed that the system in (1) does not escape to infinity during the time interval $[t_0, t_0 + \bar{\tau}]$, where $\bar{\tau} \in \mathbb{R}$ is a known positive constant defined as an upper bound of the input delay.

III. Control Development

The objective is to design a controller that enables the knee-joint angle $q(t)$ to track a given reference trajectory $q_r(t)$ despite an unknown time-varying input delay and uncertainties in the dynamic model subjected to additive bounded disturbances. To facilitate the subsequent analysis, a measurable auxiliary tracking error, denoted by $e_1 \in \mathbb{R}$, is defined as[1]

$$e_1 \triangleq \int_{t_0}^{t} (q_r(\theta) - q(\theta))d\theta. \tag{2}$$

To facilitate the subsequent analysis, an auxiliary tracking error, denoted by $e_2 \in \mathbb{R}$, is defined as

$$e_2 \triangleq \dot{e}_1 + \alpha e_1 \tag{3}$$

where $\alpha \in \mathbb{R}$ is a positive, constant control gain. To facilitate the subsequent analysis, a measurable auxiliary tracking error, denoted by $r \in \mathbb{R}$, is defined as

$$r \triangleq \dot{e}_2 + \beta e_2 + \eta e_u \tag{4}$$

where $\beta, \eta \in \mathbb{R}$ are known, positive, constant control gains. To incorporate a delay-free input term in the closed-loop error system, an auxiliary error signal, denoted by $e_u \in \mathbb{R}$, is defined as

$$e_u \triangleq -\int_{t-\hat{\tau}}^{t} u(\theta)d\theta. \tag{5}$$

By multiplying the time derivative of (4) by M and using (1)–(3) and (5), the open-loop dynamics for r can be obtained as

$$\begin{aligned} M(q,\dot{q})\dot{r} =\ & M(q,\dot{q})\ddot{q}_r + f(q,\dot{q}) + d + M(q,\dot{q})(\alpha+\beta)\dot{e}_2 \\ & - M(q,\dot{q})\alpha^2\dot{e}_1 + u_{\hat{\tau}} - u_\tau \\ & + (M(q,\dot{q})\eta - 1)u_{\hat{\tau}} - M(q,\dot{q})\eta u. \end{aligned} \tag{6}$$

Based on (6) and the subsequent stability analysis, a continuous controller is designed as

$$u = k_c r \tag{7}$$

where $k_c \in \mathbb{R}$ is a positive, constant control gain. Substituting (7) into (6), and then segregating the resulting expression into terms that can be upper bounded by a constant and terms that can be upper bounded by a state-dependent function yields

$$\begin{aligned} M(q,\dot{q})\dot{r} =\ & \tilde{N} + N_r - \frac{1}{2}\dot{M}(q,\dot{q},\ddot{q})r - e_2 + u_{\hat{\tau}} - u_\tau \\ & + (M(q,\dot{q})\eta - 1)k_c r_{\hat{\tau}} - M(q,\dot{q})\eta k_c r \end{aligned} \tag{8}$$

[1]The control objective can be quantified in terms of the first time derivative of e_1.

where the auxiliary terms $\tilde{N}, N_r \in \mathbb{R}$ are defined as

$$\begin{aligned} \tilde{N} \triangleq\ & (M(q,\dot{q}) - M(q_r,\dot{q}_r))\ddot{q}_r + f(q,\dot{q}) - f(q_r,\dot{q}_r) \\ & + M(q,\dot{q})(\alpha+\beta)\dot{e}_2 - M(q,\dot{q})\alpha^2\dot{e}_1 \\ & + \frac{1}{2}\dot{M}(q,\dot{q},\ddot{q})r + e_2 \end{aligned} \tag{9}$$

$$N_r \triangleq d + M(q_r,\dot{q}_r)\ddot{q}_r + f(q_r,\dot{q}_r). \tag{10}$$

The auxiliary term N_r in (10) is upper bounded by a known constant based on Assumptions 1–3 as

$$\sup_{t\in\mathbb{R}} |N_r| \leq \Phi \tag{11}$$

where $\Phi \in \mathbb{R}$ is a known positive constant, and from Assumption 1, an upper bound for (9) can be developed as

$$|\tilde{N}| \leq \rho(\|z\|)\|z\| \tag{12}$$

where ρ is a positive, radially unbounded, and strictly increasing function, and $z \in \mathbb{R}^4$ is a vector of error signals defined as $z \triangleq [\, e_1\ e_2\ r\ e_u \,]^T$. Based on (8) and the subsequent stability analysis, let the functions $Q_1,\ Q_2 : \mathbb{R} \to \mathbb{R}$ be defined as

$$Q_1 \triangleq \omega_1 k_c \varepsilon_1 \int_{t-\hat{\tau}}^{t} |r(\theta)|^2 d\theta \tag{13}$$

$$Q_2 \triangleq \frac{\omega_2 k_c}{\hat{\tau}} \int_{t-\hat{\tau}}^{t}\int_{s}^{t} |r(\theta)|^2 d\theta ds \tag{14}$$

and let $y \in \mathbb{R}^6$ be defined as $y \triangleq [\, z, \sqrt{Q_1}, \sqrt{Q_2}\,]^T$. Let $\mathscr{D} \subset \mathbb{R}^6$ be an open and connected set restricted by $\|z(\bullet)\| < \gamma$, $\forall \bullet \in [t_0, t]$, and the set of initial conditions $\mathcal{S}_{\mathscr{D}} \subset \mathscr{D}$ is defined as

$$\mathcal{S}_{\mathscr{D}} \triangleq \left\{ y \in \mathbb{R}^6 |\ \|y\| < \sqrt{\frac{\lambda_1}{\lambda_2}} \inf\left\{ \rho^{-1}\left(\left(\sqrt{\frac{2\sigma \underline{m}\eta k_c}{9}}, \infty\right)\right)\right\}\right\} \tag{15}$$

where $\lambda_1 \triangleq \min\{(1/2), (\underline{m}/2), (\omega_1/2)\}$ and $\lambda_2 \triangleq \max\{1, (\bar{m}/2), (\omega_1/2)\}$.[2] The following theorem is included to indicate the conditions for which uniformly ultimately bounded limb tracking is obtained.

IV. Stability Analysis

To facilitate the subsequent stability analysis, several terms are introduced. Specifically, auxiliary bounding positive constants σ , $\delta \in \mathbb{R}$ are defined as

$$\begin{aligned} \sigma \triangleq \min & \left\{ \left(\alpha - \frac{1}{2}\right), \left(\beta - \frac{1}{2} - \frac{\varepsilon_2\eta^2}{2}\right)\frac{1}{9}\underline{m}\eta k_c, \right. \\ & \left. \left(\frac{\omega_2}{3\hat{\tau}^2 k_c} - \left(\frac{\omega_1 k_c}{\varepsilon_1} + \frac{1}{2\varepsilon_2}\right)\right)\right\} \end{aligned} \tag{16}$$

$$\delta \triangleq \min\left\{ \frac{\sigma}{2}, \frac{\omega_2}{3\hat{\tau}\omega_1\varepsilon_1}, \frac{1}{3\hat{\tau}} \right\} \tag{17}$$

where $\omega_1, \omega_2, \varepsilon_1, \varepsilon_2 \in \mathbb{R}$ are known, adjustable, positive constants.

[2]For Set A, the inverse image $\rho^{-1}(A)$ is defined as $\rho^{-1}(A) \triangleq \{a \mid \rho(a) \in A\}$

Theorem 1: Given the dynamics in (1), the controller given in (7) ensures uniformly ultimately bounded tracking in the sense that

$$|q_r - q| \le \Gamma_0 \exp(-\Gamma_1(t - t_0)) + \Gamma_2 \tag{18}$$

where $\Gamma_0 \triangleq (1+\alpha)(2V(t_0) - (2\lambda_2 \upsilon/\delta))^{1/2}$, $\Gamma_1 \triangleq -(\delta/2\lambda_2)$, and $\Gamma_2 \triangleq (1+\alpha)(2\lambda_2\upsilon/\delta)^{1/2}$ with $\upsilon \triangleq ((9\Phi^2/4\underline{m}\eta) + \bar{\bar{\tau}}\Upsilon^2/k_c)$ and $\Upsilon \in \mathbb{R}$ is a positive constant[3] provided $y(t_0) \in \mathcal{S}_{\mathscr{D}}$ and the control gains are selected sufficiently large relative to the initial conditions of the system such that the following sufficient conditions are satisfied[4]

$$\begin{aligned} &\alpha > \frac{1}{2}, \quad \beta > \frac{1+\varepsilon_2\eta^2}{2} \\ &\omega_2 > \frac{3}{2}\hat{\tau}^2 k_c \left(\frac{2\omega_1 k_c}{\varepsilon_1} + \frac{1}{\varepsilon_2}\right) \\ &(M\eta - 1) \le \varepsilon_1\omega_1, \quad \frac{\frac{8\underline{m}\eta}{3} - 8\omega_1\varepsilon_1 - 4\omega_2}{k_c^2} \ge \bar{\bar{\tau}}. \end{aligned} \tag{19}$$

Proof: Let $V : \mathscr{D} \to \mathbb{R}$ be a Lyapunov function candidate defined as

$$V \triangleq \frac{1}{2}e_1^2 + \frac{1}{2}e_2^2 + \frac{1}{2}Mr^2 + \frac{\omega_1}{2}e_u^2 + Q_1 + Q_2. \tag{20}$$

The Lyapunov function candidate (20) can be bounded as

$$\lambda_1\|y\|^2 \le V(y) \le \lambda_2\|y\|^2. \tag{21}$$

Using (2)–(5) and (8), and by applying the Leibniz rule for (13)–(14), the time derivative of (20) can be determined as

$$\begin{aligned} \dot{V} =\; & e_1(e_2 - \alpha e_1) + e_2(r - \beta e_2 - \eta e_u) \\ & + \frac{1}{2}\dot{M}r^2 + r\left(\tilde{N} + N_r - \frac{1}{2}\dot{M}r - e_2 - M\eta k_c r\right) \\ & + r((M\eta - 1)k_c r_{\hat{\tau}} + (u_{\hat{\tau}} - u_\tau)) \\ & + \omega_1 e_u(k_c r_{\hat{\tau}} - k_c r) + \omega_1 k_c \varepsilon_1\left(r^2 - r_{\hat{\tau}}^2\right) \\ & + \frac{\omega_2 k_c}{\hat{\tau}}\left(\hat{\tau}r^2 - \int_{t-\hat{\tau}}^{t} r(\theta)^2\, d\theta\right). \end{aligned} \tag{22}$$

Using (11) and (12) and canceling common terms in (22), an upper bound for (22) can be obtained as

$$\begin{aligned} \dot{V} \le\; & |e_1e_2| - \alpha e_1^2 - \beta e_2^2 + \eta\,|e_2e_u| + |r|\,\rho(\|z\|)\,\|z\| \\ & + |r|\,\Phi - M\eta k_c r^2 + k_c\varepsilon_1\omega_1\,|r r_{\hat{\tau}}| + k_c\,|r\,(r_{\hat{\tau}} - r_\tau)| \\ & + \omega_1 k_c\,(|e_u r_{\hat{\tau}}| + |e_u r|) + (\omega_1 k_c \varepsilon_1)\left(r^2 - r_{\hat{\tau}}^2\right) \\ & + \frac{\omega_2 k_c}{\hat{\tau}}\left(\hat{\tau}r^2 - \int_{t-\hat{\tau}}^{t} r(\theta)^2\, d\theta\right). \end{aligned} \tag{23}$$

[3]Provided $\|z(\bullet)\| < \gamma, \forall \bullet \in [t_0, t]$ and using (7) and (8), it can be concluded that $\dot{r} < \Upsilon$, where $\gamma \in \mathbb{R}$ is a positive constant.

[4]From Assumption 1, ε_1 and ω_1 can be selected sufficiently large such that $(M\eta - 1) \le \varepsilon_1\omega_1$.

Using Young's Inequality, the following inequalities can be obtained

$$|e_1e_2| \le \frac{1}{2}e_1^2 + \frac{1}{2}e_2^2 \tag{24}$$

$$|e_2e_u| \le \frac{1}{2\varepsilon_2\eta}e_u^2 + \frac{\varepsilon_2\eta}{2}e_2^2 \tag{25}$$

$$|r r_{\hat{\tau}}| \le \frac{1}{2}r^2 + \frac{1}{2}r_{\hat{\tau}}^2 \tag{26}$$

$$|e_u r_{\hat{\tau}}| \le \frac{1}{2\varepsilon_1}e_u^2 + \frac{\varepsilon_1}{2}r_{\hat{\tau}}^2 \tag{27}$$

$$|e_u r| \le \frac{1}{2\varepsilon_1}e_u^2 + \frac{\varepsilon_1}{2}r^2. \tag{28}$$

After completing the squares for r and substituting (7) and (24)–(28) into (23), the following upper bound can be obtained:

$$\begin{aligned} \dot{V} \le\; & -\left(\alpha - \frac{1}{2}\right)e_1^2 - \left(\beta - \frac{1}{2} - \frac{\varepsilon_2\eta^2}{2}\right)e_2^2 - \frac{1}{9}\underline{m}\eta k_c r^2 \\ & + \left(\frac{\omega_1 k_c}{\varepsilon_1} + \frac{1}{2\varepsilon_2}\right)e_u^2 + \frac{9}{4\underline{m}\eta k_c}\rho^2(\|z\|)\|z\|^2 + \frac{9}{4\underline{m}\eta k_c}\Phi^2 \\ & - k_c\left(\frac{2\underline{m}\eta}{3} - 2\omega_1\varepsilon_1 - \omega_2\right)r^2 + k_c\,|r\,(r_{\hat{\tau}} - r_\tau)| \\ & - \frac{\omega_2 k_c}{\hat{\tau}}\int_{t-\hat{\tau}}^{t} r(\theta)^2 d\theta. \end{aligned} \tag{29}$$

The Cauchy–Schwarz inequality is used to develop an upper bound for e_u^2 such that $e_u^2 \le \hat{\tau}\int_{t-\hat{\tau}}^{t} u(\theta)^2 d\theta$. In addition, an upper bound for Q_2 can be obtained as $Q_2 \le \omega_2 k_c \int_{t-\hat{\tau}}^{t} r(\theta)^2 d\theta$. Using these developed upper bounds for e_u^2, Q_1, Q_2 , the following upper bound can be developed:

$$\begin{aligned} \dot{V} \le\; & -\left(\alpha - \frac{1}{2}\right)e_1^2 - \left(\beta - \frac{1}{2} - \frac{\varepsilon_2\eta^2}{2}\right)e_2^2 - \frac{1}{9}\underline{m}\eta k_c r^2 \\ & - \left(\frac{\omega_2}{3\hat{\tau}^2 k_c} - \left(\frac{\omega_1 k_c}{\varepsilon_1} + \frac{1}{2\varepsilon_2}\right)\right)e_u^2 - \frac{\omega_2}{3\hat{\tau}\omega_1\varepsilon_1}Q_1 \\ & - \frac{1}{3\hat{\tau}}Q_2 + \frac{9}{4\underline{m}\eta k_c}\rho^2(\|z\|)\,\|z\|^2 + \frac{9}{4\underline{m}\eta k_c}\Phi^2 \\ & + k_c\,|r\,(r_{\hat{\tau}} - r_\tau)| - k_c\left(\frac{2\underline{m}\eta}{3} - 2\omega_1\varepsilon_1 - \omega_2\right)r^2. \end{aligned} \tag{30}$$

Based on the definition of σ in (16), the gain conditions in (19), the inequality $\|y\| \ge \|z\|$, and the mean value theorem $|r_{\hat{\tau}} - r_\tau| \le |\dot{r}(\Theta(t, \hat{\tau}))||\tilde{\tau}|$, where $\Theta(t, \hat{\tau})$ is a point between $t - \tau$ and $t - \hat{\tau}$. Completing the squares for r, the following upper bound can be obtained:

$$\begin{aligned} \dot{V} \le\; & -\left(\frac{\sigma}{2} - \frac{9}{4\underline{m}\eta k_c}\rho^2(\|y\|)\right)\|z\|^2 - \frac{\sigma}{2}\,\|z\|^2 \\ & + \frac{9\Phi^2}{4\underline{m}\eta k_c} + \frac{\bar{\bar{\tau}}|\dot{r}(\Theta(t, \hat{\tau}))|^2}{k_c} - \frac{\omega_2 Q_1}{3\hat{\tau}\omega_1\varepsilon_1} - \frac{Q_2}{3\hat{\tau}}. \end{aligned} \tag{31}$$

Provided $y \in \mathscr{D}$ and then by using the definition of δ in (17), the inequality in (31) can be expressed as

$$\dot{V} \le -\delta\|y\|^2 + \upsilon \tag{32}$$

which after using (21) and (22) can be solved to yield

$$V(t) \le \left(V(t_0) - \frac{\lambda_2\upsilon}{\delta}\right)\exp\left(-\frac{\delta}{\lambda_2}(t - t_0)\right) + \frac{\lambda_2\upsilon}{\delta}. \tag{33}$$

TABLE I
DEMOGRAPHICS OF PARTICIPANTS WITH AN NC

Participant	Age	Sex	Injury	Months Since Injury
A	63	M	PD	233
B	25	M	SB L5-S1	Since Birth
C	33	F	SCI (T12)	51

Using (20) and (33), e_1, e_2, r, e_u can be upper bounded by exponential terms. Likewise, the exponential bound in (18) can be developed provided $y(t_0) \in \mathcal{S}_{\mathcal{D}}$. Since e_1, e_2, r, $e_u \in \mathcal{L}_\infty$, from (7), $u \in \mathcal{L}_\infty$ and the remaining signals are bounded. ■

V. EXPERIMENTS

The performance of the controller in (7) was examined through a series of experiments with healthy individuals and participants with NCs. Surface electrical stimulation was applied to the quadriceps muscle group to elicit contractions during knee-joint angle tracking trials. For all trials, the control algorithm in (7) was used to vary the current amplitude in real time, while the pulsewidth (PW) and stimulation frequency were set to constant values.

A. Participants

Ten able-bodied individuals (nine male, one female, aged 21–31, labeled S1–S10) participated in the experiments. Participants with NCs (two male, one female, labeled A–C) were recruited through the UF Health Integrated Data Repository (UF Consent2Share project) and completed the NMES protocol at the University of Florida. Demographics of the participants with NCs are listed in Table I. The participants with NCs were medically stable, met the inclusion criteria, and self-reported their motor function and mobility status. Prior to participation, written informed consent was obtained from all participants, as approved by the institutional review board at the University of Florida. The able-bodied participants were instructed to avoid voluntarily contributing to the leg extension task (i.e., to remain passive). The able-bodied individuals were not informed of nor could see the outcomes of the tracking objective of the NMES protocol. The participants with NCs were informed of the objective of the leg extension task, but no feedback regarding their performance was provided during the experiments (i.e., none of the study participants were shown the desired or actual trajectories of the leg extension task). Participant A is a participant with Parkinson's disease (PD), Modified Hoehn & Yahr Stage 3) and presented tremor in his lower and upper extremities. Participant B is a participant with Spina Bifida (SB) (level L5-S1) and Arnold Chiari malformation. Participant B uses a wheelchair part-time for mobility and a walker for ambulation at home. Participant C is a participant with SCI (lesion level T12). Participant C uses a wheelchair part-time for long-distance mobility and canes for short-distance ambulation.

B. Methods

The experimental testbed, shown in Fig. 1, consists of the following: 1) a modified leg extension machine equipped

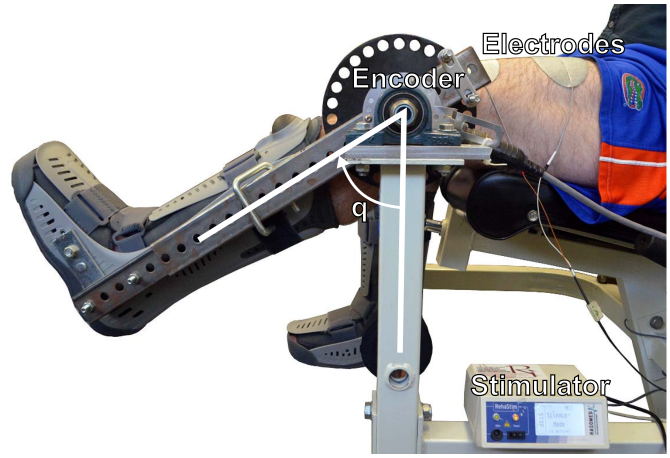

Fig. 1. Modified leg extension machine was fit with optical encoders to measure the knee-joint angle q.

with orthotic boots to fix the ankle and securely fasten the shank and the foot; 2) optical encoders (BEI Technologies) to measure the leg angle; 3) a current-controlled eight-channel stimulator (RehaStim, Hasomed GmbH); 4) a data acquisition board (Quanser QPIDe); 5) a desktop computer running MATLAB/Simulink 2015b with a sampling frequency of 1 kHz; and 6) a pair of 3" by 5" Valutrode surface electrodes placed proximally and distally over the quadriceps muscle group.[5]

During the experiments, electrical pulses were delivered at a constant stimulation frequency of 35 Hz and the PW was fixed to a constant value that depended on the individual.[6] The control gains were adjusted during pretrial tests to achieve trajectory tracking where the desired angular trajectory of the knee joint was selected as a sinusoid with a range of 5° to 50° and a period of 2 s. The constant estimate of the time-varying delay was selected as $\hat{\tau} \in [0.085, 0.12]$ s based on the results reported in previous NMES studies [6], [34], [39]. A pretrial test was conducted for each participant to acclimate him/her to the stimulation sensation and determine suitable control gains to optimize performance during the leg extension task. The tracking trial was executed for one of the lower limbs for a testing duration of between 45 and 50 s. The control performance was evaluated by calculating the root-mean-square (rms) tracking error over the entire trial. The experiment duration ranged between 45 and 60 s. Then, the process was repeated for the other lower limb starting with the pretrial tests.[7] The control gains introduced in (3), (4),

[5]Surface electrodes for the study were provided compliments of Axelgaard Manufacturing Co., Ltd.

[6]Different responses to stimulation were obtained when testing across participants (i.e., a greater or weaker muscle force was produced for a nominal stimulation intensity). Although the main gain k_c can be decreased/increased to compensate for stronger/weaker responses, the stimulator has a finite resolution. Therefore, the constant value of PW was either reduced or increased so that the resulting control input would be within an acceptable range. PW values for each individual are given in Table II. In addition, other factors were considered for modifying the PW, such as tracking accuracy and stimulation sensitivity of the healthy individuals and participants with NCs.

[7]For Participant C, tracking results were obtained only for the right-hand-side leg, because the left leg was too sensitive to stimulation to execute the experiment.

TABLE II

TRACKING RESULTS FOR HEALTHY INDIVIDUALS AND PARTICIPANTS WITH NCS QUANTIFIED BY THE rms ERROR (DEGREES). THE ESTIMATE OF DELAY AND SELECTED PW ARE ALSO LISTED FOR EACH PARTICIPANT

Participant	Leg	RMS Error (deg.)	$\hat{\tau}$(ms)	PW(μs)
S1	R	3.31	85	200
	L	4.38	85	200
S2	R	3.37	95	400
	L	3.54	95	400
S3	R	3.69	100	400
	L	3.24	100	300
S4	R	4.15	100	200
	L	4.35	100	200
S5	R	3.46	95	200
	L	4.10	95	200
S6	R	4.58	100	500
	L	4.37	100	500
S7	R	3.52	95	200
	L	3.84	95	200
S8	R	3.22	95	200
	L	4.08	95	200
S9	R	4.16	95	200
	L	3.94	95	200
S10	R	4.15	100	300
	L	3.50	100	300
Average (S1-S10)		**3.85 $\pm$ 0.43**	**96 $\pm$ 5**	-
A	R	6.54	95	300
	L	7.31	100	300
B	R	4.37	90	200
	L	5.21	100	200
C	R	5.46	100	350
Average (A-C)		**5.78 $\pm$ 1.15**	**97 $\pm$ 4.47**	-
Combined Mean		**4.23 $\pm$ 0.99**	**96 $\pm$ 4.40**	-

and (7) were selected for the healthy participants as follows: $\alpha \in [0.5, 2]$, $\beta \in [5, 15]$, $\eta \in [0.45, 0.5]$, and $k_c \in [11, 35]$.

C. Results

The leg extension tasks were successfully completed by all the enrolled participants. Table II presents the mean rms error, the selected delay estimate $\hat{\tau}$, and the PW used for each participant. Fig. 2 shows the tracking performance and the control inputs during a complete dynamic tracking trial for Participants S1 and A. Fig. 3 shows the tracking performance and the control inputs for Participants B and C.

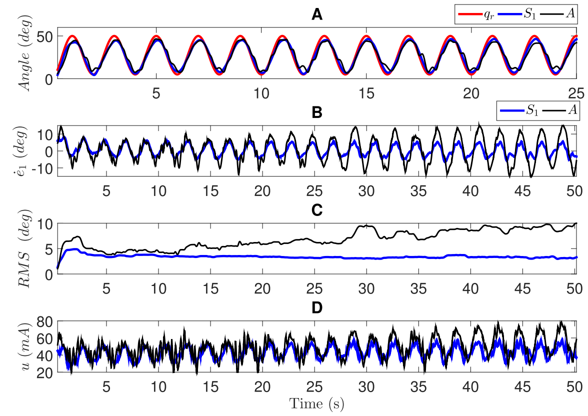

Fig. 2. Tracking performance and control inputs for Participants S1 and A (right-hand-side leg tracking). (a) Desired trajectory q_r (red line) and actual leg angle for Participants S1 (blue line) and A (black line) during the first 25 s of the experiment. (b) Angle tracking error for both the participants. (c) RMS tracking error for both the participants using a time window interval of 1.2 s. (d) Stimulation current amplitude for both the participants.

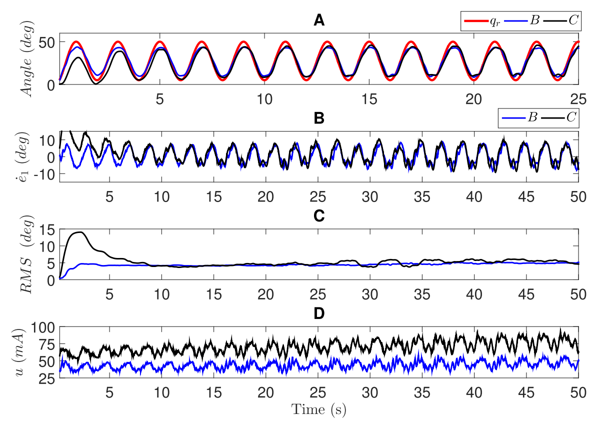

Fig. 3. Tracking performance and control inputs for Participants B and C (right-hand-side leg tracking). (a) Desired trajectory q_r (red line) and actual leg angle for Participants B (blue line) and C (black line) during the first 25 s of the experiment. (b) Angle tracking error for both the participants. (c) RMS tracking error for both participants using a time window interval of 1.2 s. (d) Stimulation current amplitude for both participants.

VI. DISCUSSION

The experimental results demonstrate the feasibility of the controller in (7) to track a desired knee-joint reference trajectory via NMES of the quadriceps muscle group. The mean rms position error is $4.23° \pm 0.99$ across the able-bodied individuals and participants with NCs. The tracking error remained bounded through the duration of the experiments despite the presence of muscle fatigue and norm-bounded disturbances. Figs. 2–3 contrast the tracking differences between an able-bodied individual and the three participants with NCs. Fig. 2(c) shows the rms error for Participants S1 and A. As a result of muscle fatigue, the tracking performance of Participant A degrades over time resulting in larger stimulation amplitudes than the healthy individual. Fig. 3 shows similar tracking performance between Participants B and C after 10 s from the onset of the experiment. The transient response of Participant C showed the largest error during the first 10 s of the experiment indicating a slower muscle response to stimulation than other participants. Hence, Participant C required consistently larger stimulation amplitudes than Participant B, as shown in Fig. 3(d), to achieve the tracking objective. Nevertheless, the tracking performance of Participant C in the steady state is similar to Participant B [see Fig. 3(c)]. Despite the fact that the controller in (7) used a constant estimate of the input delay (see Table II for the estimate values chosen for each participant), the experimental results show robustness to the unknown delay. The time delay estimates used for the experiments agree with values described in the literature for NMES isometric torque tracking [39].

The tracking results of the present work are similar to the ones obtained in [34], where a mean rms error of 3.91° was reported for five able-bodied participants tracking a periodic reference. More recent results in [35] reported improved tracking performance of a periodic reference by adding an integral control term to the previous developed controller in [34] with a mean rms error of 2.73° for four healthy test individuals. However, the results in [34] and [35] were obtained using a predictor-based approach with the assumption that the time delay was known and constant (i.e., the time delay was measured in experiments) for shorter experiment durations compared with the results presented in this brief. Further, the controller designed in this brief does not require an exact model knowledge of the neuromuscular system, the estimation of the muscle torque effectiveness, and the implementation of an online algorithm to compute the input delay compared with [39].

Additional challenges were evident in the experiments with participants with NCs. Participant C (participant with SCI) required high stimulation intensities throughout the entire experiment, as shown in Fig. 3 due to the lack of muscle strength and mass. During experiments with Participant A, tremors due to PD along with muscle fatigue show factors that resulted in suboptimal tracking compared with the results obtained from healthy individuals and Participants B and C. Nevertheless, the designed controller was able to modify the stimulation amplitude to allow the participants to complete the tracking task.

Future work will seek to incorporate a time-varying estimate of the input delay to the control structure. In addition, the extension of the current control framework to multi-muscle coordinate tasks such as cycling or the activation of antagonistic muscles as in [36] is the focus of future research efforts.

VII. Conclusion

A delay-compensating controller for NMES was designed to provide limb tracking for uncertain lower limb dynamics subject to bounded unknown additive disturbances with an unknown time-varying input delay. An auxiliary tracking error signal was designed to inject a delay-free control signal in the closed-loop dynamics without measuring the time-varying input delay. Lyapunov–Krasovskii functionals are used in the Lyapunov-based stability analysis to provide uniformly ultimate bounded lower limb tracking. Experiments were conducted in healthy individuals and participants with NCs to validate the efficacy of the developed control methods. Future efforts could extend this research by using an estimated time-varying delay in the control design instead of using a constant estimated delay to achieve more precise tracking of reference limb movement. While this brief provides new insights into compensating for the unknown-time-varying nature of the delay, additional methods could also be pursued in a production FES system to mitigate or compensate for the delay. For example, depending on the therapeutic goal, some desired trajectories could include brief pauses that inject isometric contractions that allow the delay to be measured in real-time and used in the control design. Different modulation strategies could also be pursued to implement the controller. For example, lower frequency stimulation reduces the onset of fatigue, which is linked to increased delay. The desire for lower frequency stimulation and reduced fatigue is the motivation for asynchronous stimulation strategies [52], [53]. Along these lines, pulse amplitude and PW could be simultaneously adjusted rather than fixing the PW and adjusting the amplitude as in this brief. This approach has been shown to reduce fatigue [54]. Moreover, since the mathematical model assumes the relationship between stimulation intensity and muscle force is unknown and time-varying, the control design need not be altered if the user wishes to simultaneously modulate pulse amplitude and PW.

Acknowledgment

Any opinions, findings, and conclusions or recommendations expressed in this material are those of the authors and do not necessarily reflect the views of the sponsoring agency.

References

[1] Q. Wang, "Lyapunov-based neuromuscular electrical stimulation control," Ph.D. dissertation, Dept. Elect. Comput. Eng., Univ. Florida, Gainesville, FL, USA, 2012.

[2] J. Ding, A. S. Wexler, and S. A. Binder-Macleod, "A predictive fatigue model. I. Predicting the effect of stimulation frequency and pattern on fatigue," *IEEE Trans. Rehabil. Eng.*, vol. 10, no. 1, pp. 48–58, Mar. 2002.

[3] Z. Li, M. Hayashibe, C. Fattal, and D. Guiraud, "Muscle fatigue tracking with evoked EMG via recurrent neural network: Toward personalized neuroprosthetics," *IEEE Comput. Intell. Mag.*, vol. 9, no. 2, pp. 38–46, May 2014.

[4] S. U. Yavuz, A. Şendemir-Ürkmez, and K. S. Türker, "Effect of gender, age, fatigue and contraction level on electromechanical delay," *Clin. Neurophysiol.*, vol. 121, no. 10, pp. 1700–1706, Oct. 2010. doi: 10.1016/j.clinph.2009.10.039.

[5] E. Cé, S. Rampichini, L. Agnello, E. Limonta, A. Veicsteinas, and F. Esposito, "Effects of temperature and fatigue on the electromechanical delay components," *Muscle Nerve*, vol. 47, no. 4, pp. 566–576, 2013.

[6] R. J. Downey, M. Merad, E. J. Gonzalez, and W. E. Dixon, "The time-varying nature of electromechanical delay and muscle control effectiveness in response to stimulation-induced fatigue," *IEEE Trans. Neural Syst. Rehabil. Eng.*, vol. 25, no. 9, pp. 1397–1408, Sep. 2017.

[7] N. Alibeji, N. Kirsch, and N. Sharma, "An adaptive low-dimensional control to compensate for actuator redundancy and FES-induced muscle fatigue in a hybrid neuroprosthesis," *Control Eng. Pract.*, vol. 59, pp. 204–219, Feb. 2017.

[8] P. Sampson *et al.*, "Using functional electrical stimulation mediated by iterative learning control and robotics to improve arm movement for people with multiple sclerosis," *IEEE Trans. Neural Syst. Rehabil. Eng.*, vol. 24, no. 2, pp. 235–248, Feb. 2016.

[9] T. Seel, C. Wener, J. Raisch, and T. Schauer, "Iterative learning control of a drop foot neuroprosthesis—Generating physiological foot motion in paretic gait by automatic feedback control," *Control Eng. Pract.*, vol. 48, pp. 87–97, Mar. 2016.

[10] T. Seel, C. Werner, and T. Schauer, "The adaptive drop foot stimulator–multivariable learning control of foot pitch and roll motion in paretic gait," *Med. Eng. Phys.*, vol. 38, no. 11, pp. 1205–1213, Nov. 2016.

[11] K. H. Ha, S. A. Murray, and M. Goldfarb, "An approach for the cooperative control of FES with a powered exoskeleton during level walking for persons with paraplegia," *IEEE Trans Neural Syst. Rehabil. Eng.*, vol. 24, no. 4, pp. 455–466, Apr. 2016.

[12] R. Nataraj, M. L. Audu, and R. J. Triolo, "Restoring standing capabilities with feedback control of functional neuromuscular stimulation following spinal cord injury," *Med. Eng. Phys.*, vol. 42, pp. 13–25, Apr. 2017.

[13] F. E. Zajac, "Muscle and tendon: Properties, models, scaling, and application to biomechanics and motor control," *Crit. Rev. Biomed. Eng.*, vol. 17, no. 4, pp. 359–411, 1989.

[14] A. H. Vette, K. Masani, and M. R. Popovic, "Neural-mechanical feedback control scheme can generate physiological ankle torque fluctuation during quiet standing: A comparative analysis of contributing torque components," in *Proc. IEEE Int. Conf. Control Appl.*, Sep. 2008, pp. 660–665.

[15] J.-P. Richard, "Time-delay systems: An overview of some recent advances and open problems," *Automatica*, vol. 39, no. 10, pp. 1667–1694, Oct. 2003.

[16] M. A. Henson and D. E. Seborg, "Time delay compensation for nonlinear processes," *Ind. Eng. Chem. Res.*, vol. 33, no. 6, pp. 1493–1500, 1994.

[17] M. Jankovic, "Control of cascade systems with time delay–the integral cross-term approach," in *Proc. 45th IEEE Conf. Decis. Control*, Dec. 2006, pp. 2547–2552.

[18] F. Mazenc and S.-I. Niculescu, "Generating positive and stable solutions through delayed state feedback," *Automatica*, vol. 47, pp. 525–533, Mar. 2011.

[19] F. Mazenc, M. Malisoff, and T. N. Dinh, "Robustness of nonlinear systems with respect to delay and sampling of the controls," *Automatica*, vol. 49, no. 6, pp. 1925–1931, 2013.

[20] J.-Q. Huang and F. L. Lewis, "Neural-network predictive control for nonlinear dynamic systems with time-delay," *IEEE Trans. Neural Netw.*, vol. 14, no. 2, pp. 377–389, Mar. 2003.

[21] N. Sharma, S. Bhasin, Q. Wang, and W. E. Dixon, "Predictor-based control for an uncertain Euler–Lagrange system with input delay," *Automatica*, vol. 47, no. 11, pp. 2332–2342, 2011.

[22] N. Fischer, A. Dani, N. Sharma, and W. E. Dixon, "Saturated control of an uncertain nonlinear system with input delay," *Automatica*, vol. 49, no. 6, pp. 1741–1747, Jun. 2013.

[23] R. Kamalapurkar, N. Fischer, S. Obuz, and W. E. Dixon, "Time-varying input and state delay compensation for uncertain nonlinear systems," *IEEE Trans. Autom. Control*, vol. 61, no. 3, pp. 834–839, Mar. 2016.

[24] I. Chakraborty, S. Obuz, R. Licitra, and W. E. Dixon, "Control of an uncertain Euler-Lagrange system with known time-varying input delay: A pde-based approach," in *Proc. Amer. Control Conf. (ACC)*, Jul. 2016, pp. 4344–4349.

[25] I. Chakraborty, S. Obuz, and W. E. Dixon, "Control of an uncertain nonlinear system with known time-varying input delays with arbitrary delay rates," *IFAC-PapersOnLine*, vol. 49, no. 18, pp. 522–527, 2016.

[26] F. Mazenc and P.-A. Bliman, "Backstepping design for time-delay nonlinear systems," *IEEE Trans. Autom. Control*, vol. 51, no. 1, pp. 149–154, Jan. 2006.

[27] N. Bekiaris-Liberis and M. Krstic, "Robustness of nonlinear predictor feedback laws to time-and state-dependent delay perturbations," *Automatica*, vol. 49, no. 6, pp. 1576–1590, 2013.

[28] D. Bresch-Pietri and M. Krstic, "Delay-adaptive control for nonlinear systems," *IEEE Trans. Autom. Control*, vol. 59, no. 5, pp. 1203–1218, May 2014.

[29] F. Mazenc and M. Malisoff, "New control design for bounded backstepping under input delays," *Automatica*, vol. 66, pp. 48–55, Apr. 2016.

[30] M.-S. Koo and H.-L. Choi, "Non-predictor controller for feedforward and non-feedforward nonlinear systems with an unknown time-varying delay in the input," *Automatica*, vol. 65, pp. 27–35, Mar. 2016.

[31] N. Alibeji and N. Sharma, "A PID-type robust input delay compensation method for uncertain Euler–Lagrange systems," *IEEE Trans. Control Syst. Technol.*, vol. 25, no. 6, pp. 2235–2242, Nov. 2017.

[32] S. Obuz, J. R. Klotz, R. Kamalapurkar, and W. Dixon, "Unknown time-varying input delay compensation for uncertain nonlinear systems," *Automatica*, vol. 76, pp. 222–229, Feb. 2017.

[33] S. Obuz, A. Parikh, I. Chakraborty, and W. E. Dixon, "Lyapunov-based control of an uncertain Euler-Lagrange system with uncertain time-varying input delays without delay rate constraints," in *Proc. IFAC Workshop Time Delay Syst.*, 2016, pp. 141–146.

[34] N. Sharma, C. M. Gregory, and W. E. Dixon, "Predictor-based compensation for electromechanical delay during neuromuscular electrical stimulation," *IEEE Trans. Neural Syst. Rehabil. Eng.*, vol. 19, no. 6, pp. 601–611, Dec. 2011.

[35] N. Alibeji, N. Kirsch, S. Farrokhi, and N. Sharma, "Further results on predictor-based control of neuromuscular electrical stimulation," *IEEE Trans. Neural Syst. Rehabil. Eng.*, vol. 23, no. 6, pp. 1095–1105, Nov. 2015.

[36] T. Qiu, N. Alibeji, and N. Sharma, "Robust compensation of electromechanical delay during neuromuscular electrical stimulation of antagonistic muscles," in *Proc. Amer. Control Conf. (ACC)*, Jul. 2016, pp. 4871–4876.

[37] N. Alibeji, N. Kirsch, B. E. Dicianno, and N. Sharma, "A modified dynamic surface controller for delayed neuromuscular electrical stimulation," *IEEE/ASME Trans. on Mechatronics*, vol. 22, no. 4, pp. 1755–1764, Aug. 2017.

[38] I. Karafyllis, M. Malisoff, M. de Queiroz, M. Krstic, and R. Yang, "Predictor-based tracking for neuromuscular electrical stimulation," *Int. J. Robust Nonlinear Control*, vol. 25, no. 14, pp. 2391–2419, 2015.

[39] M. Merad, R. J. Downey, S. Obuz, and W. E. Dixon, "Isometric torque control for neuromuscular electrical stimulation with time-varying input delay," *IEEE Trans. Control Syst. Technol.*, vol. 24, no. 3, pp. 971–978, May 2016.

[40] R. Downey, R. Kamalapurkar, N. Fischer, and W. E. Dixon, "Compensating for Fatigue-Induced Time-Varying Delayed Muscle Response in Neuromuscular Electrical Stimulation Control," in *Recent Results on Nonlinear Delay Control Systems: In Honor of Miroslav Krstic*. New York, NY, USA: Springer, 2015, pp. 143–161.

[41] S. Obuz, R. J. Downey, A. Parikh, and W. E. Dixon, "Compensating for uncertain time-varying delayed muscle response in isometric neuromuscular electrical stimulation control," in *Proc. Amer. Control Conf. (ACC)*, Jul. 2016, pp. 4368–4372.

[42] S. Obuz, R. J. Downey, J. R. Klotz, and W. E. Dixon, "Unknown time-varying input delay compensation for neuromuscular electrical stimulation," in *Proc. IEEE Conf. Control Appl. (CCA)*, Sydney, NSW, Australia, Sep. 2015, pp. 365–370.

[43] N. Sharma, K. Stegath, C. M. Gregory, and W. E. Dixon, "Nonlinear neuromuscular electrical stimulation tracking control of a human limb," *IEEE Trans. Neural Syst. Rehabil. Eng.*, vol. 17, no. 6, pp. 576–584, Dec. 2009.

[44] E. P. Widmaier, H. Raff, and K. T. Strang, *Human Physiology: The Mechanisms of Body Function*, A. J. Vander, J. H. Sherman, and D. S. Luciano, Eds., 9th ed. New York, NY, USA: McGraw-Hill, 2004.

[45] W. L. Buford *et al.*, "Muscle balance at the knee-moment arms for the normal knee and the ACL-minus knee," *IEEE Trans. Rehabil. Eng.*, vol. 5, no. 4, pp. 367–379, Dec. 1997.

[46] J. L. Krevolin, M. G. Pandy, and J. C. Pearce, "Moment arm of the patellar tendon in the human knee," *J. Biomech.*, vol. 37, no. 5, pp. 785–788, 2004.

[47] T. Schauer *et al.*, "Online identification and nonlinear control of the electrically stimulated quadriceps muscle," *Control Eng. Pract.*, vol. 13, no. 9, pp. 1207–1219, Sep. 2005.

[48] S. Jezernik, R. G. V. Wassink, and T. Keller, "Sliding mode closed-loop control of FES: Controlling the shank movement," *IEEE Trans. Biomed. Eng.*, vol. 51, no. 2, pp. 263–272, Feb. 2004.

[49] R. Nathan and M. Tavi, "The influence of stimulation pulse frequency on the generation of joint moments in the upper limb," *IEEE Trans. Biomed. Eng.*, vol. 37, no. 3, pp. 317–322, Mar. 1990.

[50] T. Watanabe, R. Futami, N. Hoshimiya, and Y. Handa, "An approach to a muscle model with a stimulus frequency-force relationship for FES applications," *IEEE Trans. Rehabil. Eng.*, vol. 7, no. 1, pp. 12–18, Mar. 1999.

[51] Q. Wang, N. Sharma, M. Johnson, C. M. Gregory, and W. E. Dixon, "Adaptive inverse optimal neuromuscular electrical stimulation," *IEEE Trans. Cybern.*, vol. 43, no. 6, pp. 1710–1718, Dec. 2013.

[52] R. J. Downey, M. J. Bellman, H. Kawai, C. M. Gregory, and W. E. Dixon, "Comparing the induced muscle fatigue between asynchronous and synchronous electrical stimulation in able-bodied and spinal cord injured populations," *IEEE Trans. Neural Syst. Rehabil. Eng.*, vol. 23, no. 6, pp. 964–972, Nov. 2015.

[53] R. J. Downey, T.-H. Cheng, M. J. Bellman, and W. E. Dixon, "Closed-loop asynchronous neuromuscular electrical stimulation prolongs functional movements in the lower body," *IEEE Trans. Neural Syst. Rehabil. Eng.*, vol. 23, no. 6, pp. 1117–1127, Nov. 2015.

[54] R. J. Downey, M. J. Bellman, N. Sharma, Q. Wang, C. M. Gregory, and W. E. Dixon, "A novel modulation strategy to increase stimulation duration in neuromuscular electrical stimulation," *Muscle Nerve*, vol. 44, no. 3, pp. 382–387, Sep. 2011.